Phytopathology® • XXXX • XXX:X-X • https://doi.org/10.1094/PHYTO-05-20-0176-R

e-Xtra*

In Silico Identification of the Full Complement of Subtilase-Encoding Genes and Characterization of the Role of *TaSBT1.7* in Resistance Against Stripe Rust in Wheat

Yuheng Yang,[1,2,†] Fengfeng Zhang,[1] Tianyu Zhou,[3] Anfei Fang,[1] Yang Yu,[1] Chaowei Bi,[1] and Shunyuan Xiao[2,4,†]

[1] College of Plant Protection, Southwest University, Chongqing 400715, China
[2] Institute for Bioscience and Biotechnology Research, University of Maryland, Rockville, MD, 20850, U.S.A.
[3] Citrus Research Institute, Southwest University, Chongqing, 400712, China
[4] Department of Plant Science and Landscape Architecture, University of Maryland, College Park, MD 20742, U.S.A.
Accepted for publication 22 July 2020.

ABSTRACT

Plant subtilases (SBTs) or subtilisin-like proteases comprise a very diverse family of serine peptidases that participates in a broad spectrum of biological functions. Despite increasing evidence for roles of SBTs in plant immunity in recent years, little is known about wheat (*Triticum aestivum*) SBTs (TaSBTs). Here, we identified 255 *TaSBT* genes from bread wheat using the latest version 2.0 of the reference genome sequence. The SBT family can be grouped into five clades, from TaSBT1 to TaSBT5, based on a phylogenetic tree constructed with deduced protein sequences. In silico protein-domain analysis revealed the existence of considerable sequence diversification of the TaSBT family which, together with the local clustered gene distribution, suggests that *TaSBT* genes have undergone extensive functional diversification. Among those *TaSBT* genes whose expression was altered by biotic factors, *TaSBT1.7* was found to be induced in wheat leaves by chitin and flg22 elicitors, as well as six examined pathogens, implying a role for *TaSBT1.7* in plant defense. Transient overexpression of *TaSBT1.7* in *Nicotiana benthamiana* leaves resulted in necrotic cell death. Moreover, knocking down *TaSBT1.7* in wheat using barley stripe mosaic virus-induced gene silencing compromised the hypersensitive response and resistance against *Puccinia striiformis* f. sp. *tritici*, the causal agent of wheat stripe rust. Taken together, this study defined the full complement of wheat *SBT* genes and provided evidence for a positive role of one particular member, *TaSBT1.7*, in the incompatible interaction between wheat and a stripe rust pathogen.

Keywords: disease control and pest management, genetics and resistance, PAMP elicitors, plant immunity, stripe rust, subtilase, *TaSBT1.7*, wheat

Plant proteases, like those in other organisms, are believed to be dedicated to the degradation of damaged or functional proteins involved in a variety of biological processes (van der Hoorn 2008). As such, they are expected to play important regulatory roles in plant growth and development, as well as in responses to biotic and abiotic stresses via selective degradation of their substrates (Schaller et al. 2018). Proteases can be classified into four major types based on the peptide bonds they cleave: cysteine proteases, serine proteases, metalloproteases, and aspartic proteases (van der Hoorn 2008). Serine proteases, named for the nucleophilic Ser residue at the active site, are a highly abundant and functionally diverse class of proteins that have been shown to be involved in plant senescence, lignin synthesis, seed germination, cell and tissue differentiation, and programmed cell death (PCD) (Antão and Malcata 2005; Arora and Singh 2004; Xu et al. 2019).

Subtilisin-like proteases (subtilases [SBTs]) are a family of extracellular and broad-spectrum serine proteases characterized by a catalytic triad of amino acids: aspartate, histidine, and serine (Dodson and Wlodawer 1998). In plants, SBTs are especially abundant, and involved in a variety of developmental processes (Berger and Altmann 2000; D'Erfurth et al. 2012; Othman and Nuraziyan 2010; Roberts et al. 2011; Tanaka et al. 2001; Taylor and Qiu 2017; Zhao et al. 2000). In recent years, several plant SBTs have been identified to be widely involved in plant-pathogen recognition and immune priming (Cai and Gallois 2015; Figueiredo et al. 2014). Tomato SBTs P69A, P69B, and P69C were reported to be induced following infection by *Pseudomonas syringae* (Jordá et al. 1999) or Citrus exocortis viroid (Tornero et al. 1996, 1997), or application of salicylic acid (SA) (Jordá and Vera 2000). Two oat SBTs, Saspase-1 and Saspase-2, involved in the degradation of Rubisco in infected oat leaves during the oat–*Cochliobolus victoriae* incompatible interaction, were shown to exhibit caspase-like activity and, thus, were thought to play an important role in PCD associated with plant defense (Coffeen and Wolpert 2004). Likewise, StSBTc-3, a potato SBT, was also shown to cause cytoplasm shrinkage and death of plant cells in vitro, contributing to the restriction of *Phytophthora infestans* spread (Fernández et al. 2012, 2015). Furthermore, transgenic *Arabidopsis thaliana* overexpressing AtSBT3.3 showed enhanced resistance against *Pseudomonas syringae* DC3000 (Ramírez et al. 2013), whereas cotton plants with reduced *GbSBT1* expression by RNAi showed compromised resistance against Verticillium wilt (Duan et al. 2016). Those observations suggest that certain SBT family members are engaged in defense priming or defense activation in plants. However, the biological and molecular functions of most *SBT* genes in plants, especially those from agronomically important crops such as wheat, remain uncharacterized.

Bread wheat, second only to maize in grain production, is cultivated across more areas than any other cereal crop (Wulff and Dhugga 2018). Bread wheat is an allohexaploid (*Triticum aestivum*; 2n = 6x = 42; AABBDD) that originated from interspecific hybridization between three diploid progenitor species: *T. urartu*

†Corresponding authors: Y. Yang; yyh023@swu.edu.cn; and S. Xiao; xiao@umd.edu

Funding: This work was supported by the National Natural Science Foundation of China (grant 31801719), National Key R&D Program of China (2018YFD0200500), China Scholarship Council (201706995068 to Y. Yang), and Natural Science Foundation (grant IOS-1901566 to S. Xiao).

*The *e*-Xtra logo stands for "electronic extra" and indicates that supplementary tables and seven supplementary figurers are published online.

The author(s) declare no conflict of interest.

(2n = 2x = 14; AA), *Aegilops speltoides* (2n = 2x = 14; BB), and *A. tauschii* (2n = 2x = 14; DD) (The International Wheat Genome Sequencing Consortium 2014). World wheat production is constantly threatened by various diseases, especially rust. Understanding the molecular mechanisms by which wheat cultivars activate defense upon pathogen infection is instrumental to engineering novel and more effective disease resistance. Despite tremendous progress toward the molecular basis of the classical disease resistance gene-dependent immune signaling, relatively little is known about how the defense network is regulated and fine tuned by other components. As mentioned above, increasing evidence has suggested a role of plant SBTs in regulation of plant resistance against pathogens. Consistent with this notion, it has been reported that production of a putative apoplastic SBT was considered to be associated with the defense response against both heat shock stress and leaf rust infection in wheat (Fan et al. 2016). However, definitive genetic evidence has yet to be provided for a clear role of any wheat *SBT* genes in disease resistance. In this study, we identified in silico all possible SBT-encoding genes in the wheat genome, examined the expression patterns of a subset of *SBT* genes in response to pathogen infection, and obtained genetic evidence to indicate that *TaSBT1.7* plays a positive role in wheat resistance against an avirulent rust pathogen.

MATERIALS AND METHODS

Data mining. For wheat (*T. aestivum*) SBT (TaSBT) homolog retrieval, the annotated proteins in the RefSeq v2.0 database of International Wheat Genome Sequencing Consortium (IWGSC) (The International Wheat Genome Sequencing Consortium et al. 2018) were searched by using the HMM program implemented in InterMine tool (https://urgi.versailles.inra.fr/WheatMine/begin.do) and by querying the SBT family domain motif (accession number PF00082) found in the Pfam database (El-Gebali et al. 2018). The amino acid sequences of candidate *TaSBT* family genes were queried in the Pfam database for further confirming the domain structures. The chromosomal locations of *SBT* genes were generated using MapGene2Chromosome V2 (http://mg2c.iask.in/mg2c_v2.0/).

Alignment of sequences and phylogenetic analysis. A phylogenetic study was performed to study the structuration of the TaSBT family and confirm homologous groups. An unrooted phylogenetic tree was constructed based on the alignment of TaSBT amino acid sequences using the maximum-likelihood method available in MEGA7 software. Alignment was conducted using the ClustalW algorithm. Based on the homologous proteins in *Arabidopsis thaliana*, SBT members in wheat were categorized into five clusters (SBT1 to SBT5). Homology search results were then parsed, and sequences with at least 90% identity were considered duplicates. Figures that show these duplications were generated using TBtools (Chen et al. 2020).

Expression analysis of *TaSBT* genes in response to biotic stresses. The expression profiles of *TaSBT* genes in response to chitin and flg22 elicitors and six main biotic stresses (*Blumeria graminis* f. sp. *tritici*, *Fusarium graminearum*, *F. pseudograminearum*, *Magnaporthe oryzae*, *Puccinia striiformis* f. sp. *tritici*, and *Zymoseptoria tritici*) were monitored on the basis of the wheat transcript data available on the Wheat Expression Browser platform (Borrill et al. 2016). A heatmap of wheat *LysM* gene expression profiles at different induced conditions was constructed using TBtools (Chen et al. 2020).

Expression profile of *TaSBT1.7* and *TaPR1*. Primer design and reactions were conducted as described previously (Chichkova et al. 2010). The primers for quantitative reverse-transcription PCR (qRT-PCR) are listed in Supplementary Table S4. Gene profile analysis was quantified using a CFX96 real-time PCR detection system (Bio-Rad). qRT-PCR data were analyzed with the comparative $2_T^{\Delta\Delta C}$ method (Pfaffl 2001). Wheat elongation factor gene *TaEF-1a* (GenBank accession number Q03033) was used as an internal reference. Three independent biological replicates were performed, including three controls without the template.

Over-expression of *TaSBT1.7* in *Nicotiana benthamiana*. The binary overexpression vector pGR106 and *Agrobacterium tumefaciens* strain GV3101 were used for transient expression of *TaSBT1.7*. Fresh agrobacteria carrying an expression plasmid (pGR::TaSBT1.7) was grown overnight in Luria-Bertani medium. After centrifugation, bacterial pellets were resuspended in an infiltration buffer containing morpholineethanesulfonic acid at 10 mmol/liter, 1 $MgCl_2$ at 0 mmol/liter, and acetosyringone at 400 µmol/liter, and cell density was adjusted to an optimal optical density at 600 nm. Then, *Agrobacterium* GV3101 expressing pGR::TaSBT1.7 was infiltrated into *Nicotiana benthamiana* leaves. The negative control plants were agroinfiltrated with *A. tumefaciens* carrying an empty vector (pGR::106) and the positive control plants were infiltrated with *A. tumefaciens* carrying the *BAX* gene (pGR::BAX). Cell death symptoms were examined between 5 and 14 days after infiltration. Three independent biological replicates were performed.

Chemical treatment. Two-leaf-stage Su11 seedlings were sprayed (0.1 ml/plant) with SA at 2 mmol/liter, methyl jasmonate (MeJA) at 100 µmol/liter, or ethylene (ETH) at 100 µmol/liter in 0.05% Tween 20, as previously described (Wang et al. 2017). The control consisted of 0.05% Tween 20. Leaf samples were harvested at 0, 0.5, 2, 6, 12, and 24 h posttreatment.

Functional validation of predicted signal peptide. The function of the predicted signal peptide of TaSBT1.7b protein was validated as described previously (Yu et al. 2017). The initial 90-bp fragments of *TaSBT1.7b* cDNA were amplified by using the primers in Supplementary Table S4, then ligated into yeast signal trap vector pSUC2. The recombinant vector was transformed into yeast strain YTK12 using the lithium acetate method. Positive transformants were grown on CMD-W medium (0.67% yeast N base without amino acids, 0.075% tryptophan dropout supplement, 0.1% glucose, 2% sucrose, and 2% agar), then replica plated onto YPRAA medium (2% raffinose, 2% peptone, 1% yeast extract, and antimycin A at 2 µg/ml) to conduct an assay for invertase secretion. The YTK12 strain transformed with pSUC2 and an untransformed YTK12 strain were used as negative controls.

Subcellular localization assay. A p35S::TaSBT1.7b-enhanced green fluorescent protein (GFP) fusion construct was made by using the primers in Supplementary Table S4. Then, the recombinant vector was transiently transformed into 5-week-old *N. benthamiana* leaves via *Agrobacterium*-mediated transformation. After 2 days, infiltrated areas from the leaves were excised and examined by confocal microscopy using a Zeiss LSM710 microscope.

Barley stripe mosaic virus-mediated *TaSBT1.7* genes silencing in wheat. Two special fragments (named TaSBT1.7-V1 and TaSBT1.7-V2, which are identical in all three *TaSBT1.7* homeologs) were amplified using gene-specific primers (Supplementary Table S4) for gene silencing. Two specific cDNA fragments with *Nhe*I restriction sites were constructed into the original barley stripe mosaic virus (BSMV)::γ vector, as previously described (Yang et al. 2013), the constructs were designated as BSMV::TaSBT1.7-V1 and BSMV::TaSBT1.7-V2, respectively. A BLAST search of the two fragments against the GenBank database did not identify wheat genes other than *TaSBT1.7* sequences, thereby indicating the specificity of the sequence fragments. Subsequently, the capped in vitro transcripts were prepared from linearized plasmids containing the tripartite BSMV genome (Petty et al. 1990) using the RiboMAX Large-Scale RNA Production System-T7 (Promega Corp.) and the Ribo m^7G Cap Analog (Promega Corp.).

The second leaves of the two-leaf-stage wheat seedlings were inoculated with BSMV as previously described (Hein et al. 2005). After incubation for 24 h in the dark, seedlings were moved into a growth chamber at 25 ± 2°C. The fourth leaf of each plant was inoculated with urediniospores of CYR23 at 12 days after the viral

inoculation. These leaves were sampled at 0, 48, and 120 h postinoculation (hpi) for RNA extraction and expression level analysis. The infection phenotypes of stripe rust fungi were examined at 14 days postinoculation (dpi). Three independent biological replicates were performed.

Fungal biomass analysis. To quantify the fungal biomass in the VIGS plants, semiquantitative PCR was used, as previously described (Zhou et al. 2020). Approximately 0.02 g of BSMV-infected wheat leaves was ground to a fine powder with a mortar and pestle. Genomic DNA was extracted via the cetyltrimethylammonium bromide method. DNA samples were dissolved in double-distilled (dd)H_2O, quantified, and adjusted to a final concentration of 100 ng/μl. All of the DNA samples were amplified primer PstEF (Supplementary Table S4) to determine the number of amplification cycles for different samples, then amplified with CYR23-specific primers (Supplementary Table S4) according to the determined number of amplification cycles. The CYR23 DNA was used as a reference. The software Image J was used to convert the bands in agarose gel electrophoresis to gray values, and calculate the fungal biomass of each treatment. Three independent biological replicates were performed.

Pectin methylesterase activity assay. Pectin methylesterase (PME) activities were detected by Ruthenium Red staining as previously described (Saez-Aguayo et al. 2013), with appropriate modifications. In brief, total protein extracts were obtained by grinding 200 mg of wheat leaves in 400 ml of extraction buffer

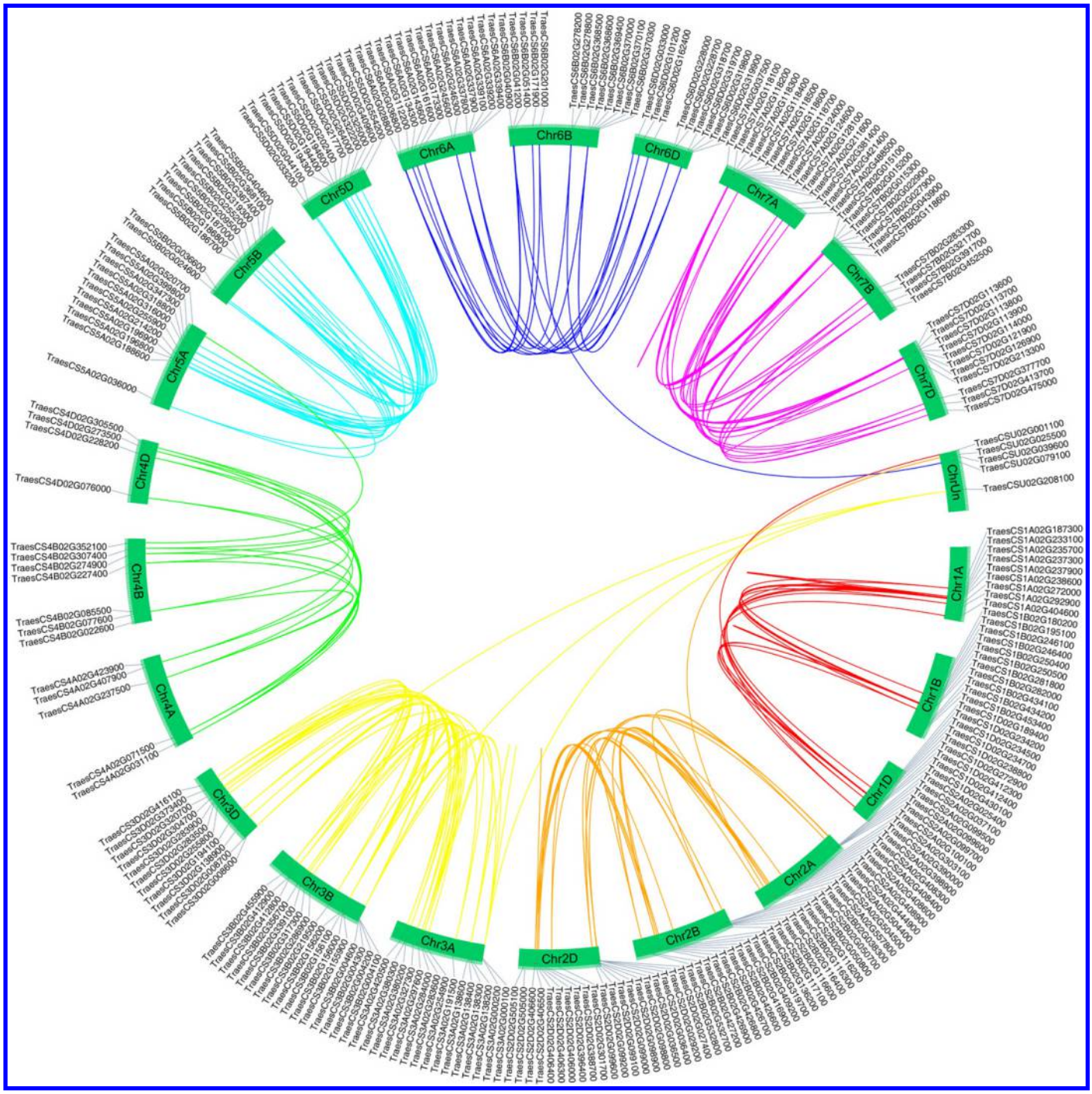

Fig. 1. Number and location of wheat subtilase (*TaSBT*) genes in the wheat genome. All 255 *TaSBT* genes were mapped to their respective locus in the wheat subgenomes in a circular diagram. Homeologous genes were inferred by phylogeny (with more than 90% of nucleotide identity), and linked with chromosome group-specific shades.

thoroughly. Obtained homogenate was shaken at 4°C for 1 h, then centrifuged at 20,000 × *g* for 15 min, and the crude proteases were obtained by retaining the supernatant. After determining the concentration, 100 µg of crude protease solution per each sample was loaded into 6-mm-diameter wells in 1% (wt/vol) agarose plates prepared with 0.1% (wt/vol) of 85% esterified citrus fruit pectin (Sigma-Aldrich). After incubating at 28°C overnight, the plates were stained with 0.05% (wt/vol) Ruthenium Red for 45 min, then decolorized with ddH_2O for 3 h. The software Image J was used to convert the stained colors in agarose plates to gray values and calculate the relative PME activities of each treatment. Three independent biological replicates were performed.

RESULTS

Genomewide in silico identification of putative SBT-encoding genes in wheat. To identify all possible SBT-encoding genes in the wheat genome, we used the SBT domain motif (PF00082) from the Pfam database as a query to search for all possible SBT-encoding genes in the latest version of the reference wheat genome released by the IWGSC. In total, 255 open reading frames predicted to encode at least one domain unique to SBTs were identified in any of the A, B, or D subgenome or unassigned chromosome (ChrUn) of *T. aestivum*. Structures of such "SBT" domains were further confirmed in the Pfam database (Supplementary Fig. S1). The predicted *SBT* genes are distributed in all wheat chromosomes (Fig. 1), with 17 tandem duplications found in chromosomes 2, 3, 5, 6, and 7 of all three subgenomes (Supplementary Fig. S1). To our knowledge, the *SBT* gene family identified in the wheat genome is the largest among those reported thus far in plants (Table 1).

Among the 255 predicted TaSBTs, 108 contain both the PA and Fn-III domains (42.4%); 127 contain the Fn-III domain but lack the PA domain (49.8%); and 3, which are encoded by a homeologous group (*TraesCS2A02G557800*, *TraesCS2B02G426700*, and *TraesCS2D02G099200*), contain the PA domain but lack the Fn-III domain. Most predicted TaSBTs (215, accounting for 84.3% of the total) contain the peptidase inhibitor I9 domain that is thought to prevent autoactivation. Consistent with the notion that most SBTs are secreted, 212 putative TaSBTs (83.1%) contain a signal peptide. Additionally, seven are predicted to contain a transmembrane structure, four with a coiled-coil structure and three with a tripeptidyl peptidase II domain (Supplementary Fig. S2).

Phylogenetic analysis of TaSBTs. To understand the evolution and sequence diversification of the TaSBT family, a phylogenetic tree based on ClustalW alignment of the amino acid sequences of all 255 predicted TaSBTs was constructed using the maximum-likelihood method. Based on the phylogenetic relationship with the *Arabidopsis thaliana* SBTs, the TaSBT family can be grouped into five clades (i.e., from TaSBT1 to TaSBT5) (Fig. 2A). Among the five clades, TaSBT2 is the largest group, with 100 members (accounting for 39.2%); followed by TaSBT3, with 65 members (accounting for 25.5%); TaSBT1, with 61 members (accounting for 23.9%); TaSBT5, with 22 members (accounting for 8.6%); and the smallest group, TaSBT4, with only 7 members (accounting for 2.7%) (Supplementary Table S1).

Interestingly, in total, 73 *TaSBT* genes reside within 1 of the 17 gene clusters where a single or multiple tandem duplication events contributed to the amplification of the *TaSBT* genes in the three wheat subgenomes (Fig. 2B; Supplementary Table S2). More specifically, eight distinct tandem duplications (TD1 to TD6, TD10, and TD11) (Fig. 2B) residing in the second or the fifth homeologous chromosomes were detected within the *TaSBT2* clade, six tandem duplications (TD7 to TD9 and TD15 to TD17) (Fig. 2B) residing in the third and seventh homeologous chromosomes were found in the *TaSBT3* clade, and three tandem duplications (TD12 to TD14) (Fig. 2B) residing in the sixth homeologous chromosomes were found in the *TaSBT1* clade. Apparently, these gene duplication events provide a huge reservoir for functional diversification and probably neofunctionalization of the prototypical *TaSBT* genes in wheat during evolution. The possession of such a large and structurally diverse SBT family in wheat suggests that SBTs play important roles in a wide range of biological processes and that many of them are probably functionally redundant.

Expression profile of *TaSBT* genes in response to phytopathogenic infection. To identify key *TaSBT* genes involved in defense activation, the expression profiles of all of the *TaSBT* genes were extracted from publicly available RNA-sequencing (RNA-seq) data obtained from leaf tissues treated with chitin or flg22, two commonly used pathogen-associated molecular patterns (PAMPs), or inoculated with one of six selected wheat pathogens (i.e., *B. graminis* f. sp. *tritici*, *F. graminearum*, *F. pseudograminearum B. graminis* f. sp. *tritici*, *F. graminearum*, *F. pseudograminearum*, *M. oryzae*, *P. striiformis* f. sp. *tritici*, and *Z. tritici*). It was found that 67 *TaSBT* genes exhibited increased expression (i.e., >4 transcripts per million) under at least one treatment, among which 27 were induced to higher levels by both chitin and flg22 (Fig. 3; Supplementary Fig. S3). The latter group include 10 homeologous genes from four *TaSBT* clades (i.e., *SBT1*, *SBT2*, *SBT3*, and *SBT5*), and the remaining are paralogous genes (belonging to the *SBT3* clade) within three tandem duplication clusters. In the case of pathogen challenges, only five homeologous genes and one gene within a tandem duplication cluster were induced to higher levels by wheat biotrophic pathogens *B. graminis* f. sp. *tritici* and *P. striiformis* f. sp. *tritici* (Fig. 3). Notably, the same four homeologous genes showed higher expression levels upon treatment with either of the two PAMP elicitors, and after pathogen infection. Interestingly, two homeologous *SBT* genes (*TraesCS5B02G036600* and *TraesCS5D02G044100*) were induced to higher levels by each and every one of the six pathogens examined (Fig. 3).

BLAST search using deduced protein sequences identified three TaSBTs homeologous groups (TraesCS6A02G143600 and TraesCS6B02G171900; TraesCS3A02G380200 and TraesCS3B02G412800; and TraesCS3A02G380300, TraesCS3B02G412900, and TraesCS3D02G373400) to be homologous (47 to 52% sequence identity) to two caspase-like proteases, *Solanum tuberosum* SBT StSBTc-3 and *N. tabacum* SBT NtPhytaspase. Likewise, one TaSBTs homeologous group (TraesCS5A02G318800, TraesCS5B02G319300,

TABLE 1. Number of subtilase (SBT) members from various plant species

Type	Subgroups[a]							Total	Reference
	SBT1	SBT2	SBT3	SBT4	SBT5	SBT6	SBT7		
Triticum aestivum	61	100	65	7	22	–	–	255	
Arabidopsis thaliana	9	6	18	15	6	2	–	56	Rautengarten et al. 2005
Lycopersicon esculentum	61	5	2	7	4	1	1	82	Reichardt et al. 2018
Oryza sativa	/	/	/	/	/	/	/	63	Tripathi and Sowdhamini 2006
Populus trichocarpa	/	/	/	/	/	/	/	90	Schaller et al. 2012
Solanum tuberosum	17	16	13	32	3	–	–	82	Norero et al. 2016
Vitis vinifera	23	4	14	13	34	6	–	97	Figueiredo et al. 2016

[a] Symbols: – indicates no SBT member identified and / indicates ungrouped.

and TraesCS5D02G325000) showed significant homology (47 to 48% sequence identity) to *A. thaliana* SBT3.3 (AT1G32960). However, these *TaSBT* genes cannot be induced by PAMPs and pathogens (Supplementary Fig. S3). Most notably, three SBT1-clade TaSBT homeologs (TraesCS4A02G237500, TraesCS4B02G077600, and TraesCS4D02G076000, with 96 to 97% nucleotide sequence identity each other) share 66% sequence identity with *A. thaliana* SBT1.7 (AT5G67360) (Supplementary Fig. S4). Thus, our subsequent functional analysis in this study was focused on *TaSBT1.7*.

***TaSBT1.7* regulates cell death and defense responses.** Previous studies suggested a role for SBT in plant defense responses. However, whether *TaSBT1.7* or its homologs in other plants indeed play a role in regulation of plant immunity remains known (Supplementary Fig. S5). To assess the importance and possible role of the *TaSBT1.7* homeologs, we examined their distribution in a range of wheat tissues. In roots and culms, expression levels of *TaSBT1.7* were found at moderate abundance. The transcripts of *TaSBT1.7* in leaves were over twofold greater than in the other tissues examined, especially for *TaSBT1.7b* (Fig. 4A). To explore whether *TaSBT1.7* is, indeed, involved in the regulation of disease resistance in wheat, the expression of the three *TaSBT1.7* homeologs in response to *P. striiformis* infection was further investigated. In wheat leaves inoculated with avirulent *P. striiformis* race CYR23, the expression levels of all three *TaSBT1.7* homeologs showed a clear upregulation between 12 and 24 hpi, then dropped back to normal at 72 hpi (Fig. 4B). Notably, *TaSBT1.7b* had the greatest (approximately sevenfold) increase at 12 hpi when compared with the control. By contrast, expression of the three *TaSBT1.7* homeologs remained low and largely unchanged after inoculation with CYR33, a virulent race of *P. striiformis* (Fig. 4B).

To test whether *TaSBT1.7* has a potential regulatory role in PCD activation, *TaSBT1.7* as a transgene was transiently overexpressed in tobacco leaves via agroinfiltration using the potato virus X delivery system. Tobacco leaves overexpressing *TaSBT1.7b* (Fig. 5) showed obvious necrotic cell death at 5 days after infiltration, although the necrosis occurred later and was milder when compared with that induced by *BAX* (which occurred at 4 days after infiltration) (Fig. 5). As a control, leaf areas infiltrated with the wild-type *Agrobacterium* strain GV3101 or a strain harboring the empty pGR106 vector did not show any sign of cell death. In addition, the expression of the three *TaSBT1.7* homeologs in wheat plants was rapidly (0.5 h) upregulated (>3.5×) upon SA treatment when compared with buffer controls, then gradually returned to the basal levels (Fig. 6). By contrast, their expression showed little or no change upon treatment with MeJA and ETH (ethephon) (Fig. 6). These results suggest that expression of the *TaSBT1.7* homoelogs above a threshold level may activate PCD in tobacco leaf tissue via the SA pathway. Protein structure prediction suggested that *TaSBT1.7* contained a signal peptide, and localized outside of the plasma membrane (Supplementary Fig. S6A). To confirm the prediction results, the function of the predicted signal peptide of *TaSBT1.7* was validated (Supplementary Fig. S6B). Subsequently, a TaSBT1.7-GFP fusion protein was expressed in tobacco leaves via agroinfiltration. As expected, TaSBT1.7-GFP showed a typical colabeling of the plasma membrane, as observed through its coexpression with propidium iodide dye (Supplementary Fig. S6C).

To determine whether *TaSBT1.7* plays a role in disease resistance in wheat, two RNAi constructs were made to specifically silence all three *TaSBT1.7* homeologs by using the BSMV-mediated gene-silencing system (Fig. 7A). All of the BSMV-inoculated plants displayed severe chlorotic mosaic symptoms at 12 dpi as a result of BSMV infection, as expected. At 12 dpi with BSMV, the fourth leaf was then inoculated with fresh urediniospores of an avirulent *P. striiformis* strain CYR23. Conspicuous hypersensitive response (HR) (Fig. 7A, arrows) was elicited by CYR23 on control leaves that were infected with BSMV::γ; however, few or no HR lesions but obvious accumulation of fungal urediniospores (arrowheads) were

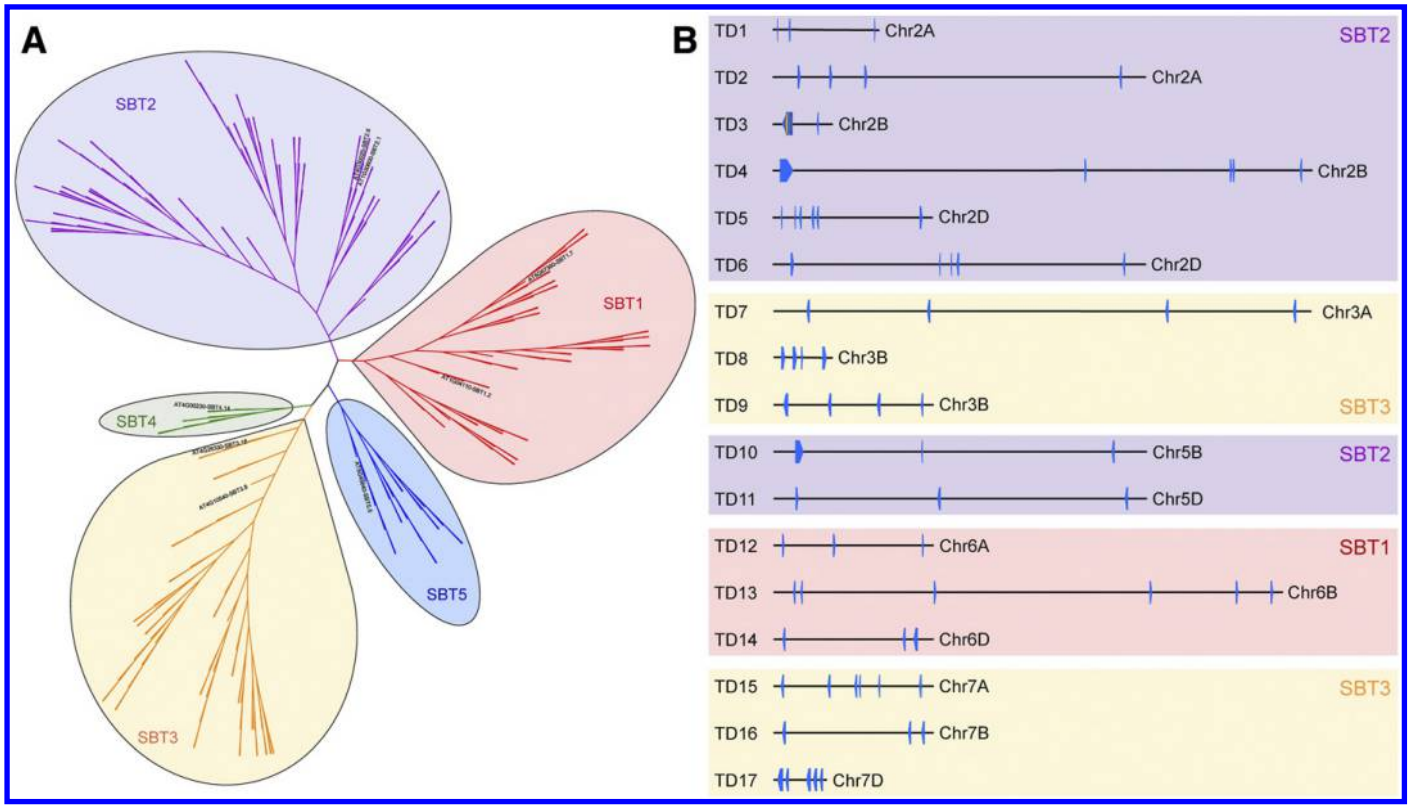

Fig. 2. Sequence diversity and chromosomal locations of wheat subtilases (TaSBTs). **A,** Deduced protein sequences of 255 TaSBTs along with nine representative AtSBTs were aligned by ClustalW and the phylogenetic tree was constructed with MEGA 5.0. Five SBT clades identified appear in different shades. **B,** Seventy-three *TaSBTs* were found to reside in 17 tandem duplication clusters found in five groups of homeologous chromosomes.

visible to the naked eye on leaves infected with BSMV::TaSBT1.7-V1 or BSMV::TaSBT1.7-V2 at 14 dpi with *P. striiformis*. To confirm whether all three *TaSBT1.7* homeologs were silenced, qRT-PCR was performed with the BSMV-infected leaves. Results showed that the expression levels of all three *TaSBT1.7* homeologs (measured by the same primer pair) were reduced to only approximately 30% of that in the control leaves before and after infection by the fungal pathogen (Fig. 7B). These results suggest that the three

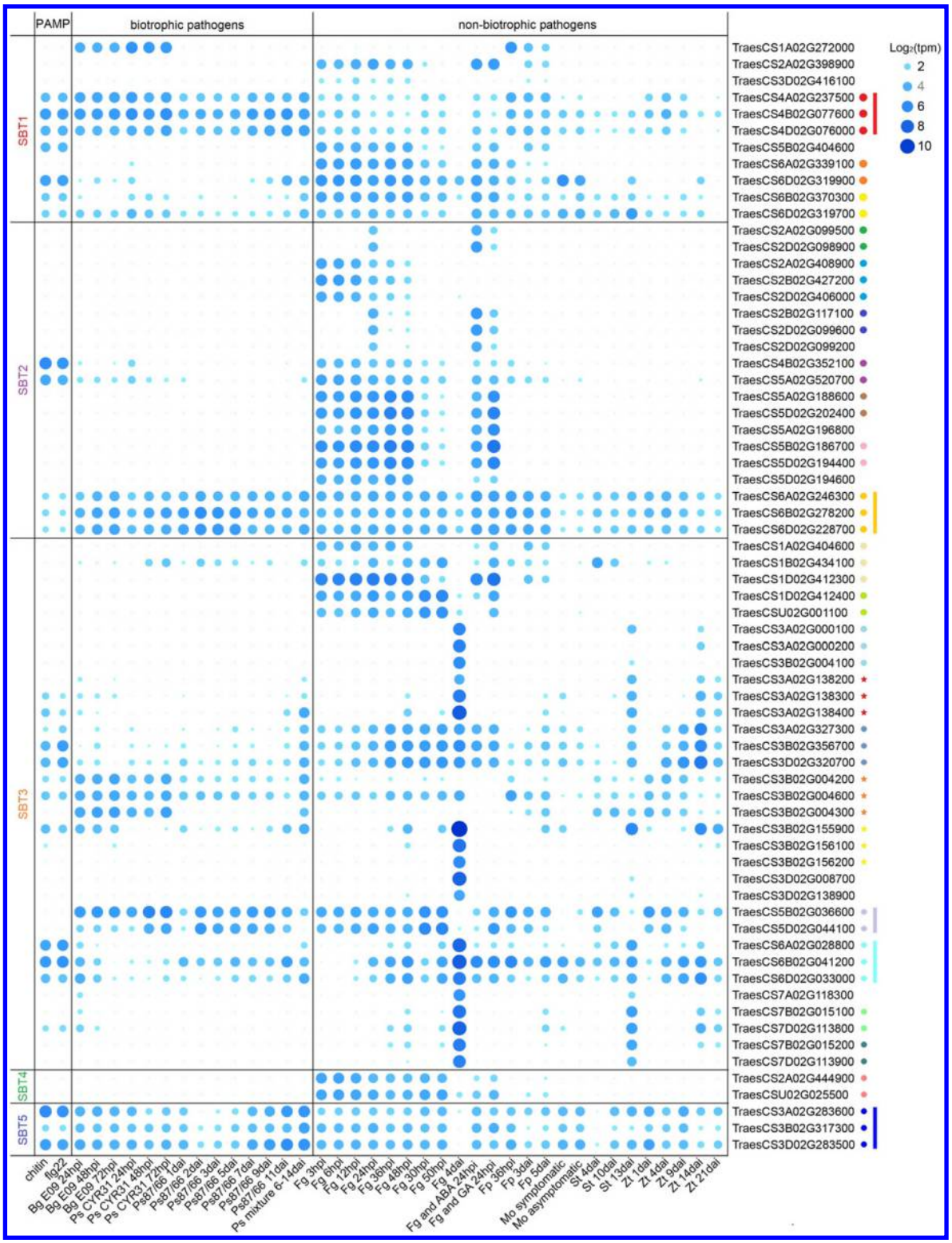

Fig. 3. Expression profiles of 67 wheat subtilase (*TaSBT*) genes upon treatment with chitin or flg22, or infection by one of six wheat pathogens based on publicly available RNA sequencing data. PAMP = pathogen-associated molecular pattern. Different shades correspond to $\log_2$ transformed transcripts per million values (for details, see Materials and Methods). Light shades denote low levels of expression, whereas dark shades denote high levels of expression. Bg = *Blumeria graminis* f. sp. *tritici*, Fg = *Fusarium graminearum*, Fp = *F. pseudograminearum*, Mo = *Magnaporthe oryzae* = Ps = *Puccinia striiformis* f. sp. *tritici*, Zt = *Zymoseptoria tritici* (synonym *Septoria tritici* = St), hpi = hours postinoculation, and dai = days after inoculation. Dots or stars in the same shade on the left side of gene IDs represent homeologous groups or tandem duplications. Shaded stripes beside the dots indicate all three homeologous genes that exhibited similar induction patterns with most of the treatments.

TaSBT1.7 homeologs may be required for full expression of the HR and resistance in wheat during its incompatible interaction with *P. striiformis*. Interestingly, the transcripts of *TaPR1* (marker gene in the SA pathway) were significantly suppressed when *TaSBT1.7* knocked down plants inoculated with avirulent strain CYR23, which helps explaining why *TaSBT1.7*-silenced plants are compromised in disease resistance.

To further characterize the degree of reduced defenses at the cellular and subcellular levels in *TaSBT1.7*-silenced plants, leaf segments from at least three BSMV-infected plants inoculated with CYR23 at 48 and 120 hpi were subjected to microscopic examination. Substomatal vesicles (Fig. 7C, SV) appeared in plants infected with either BSMV::γ, BSMV::TaSBT1.7-V1, or BSMV::TaSBT1.7-V2 at 48 hpi. However, the area of necrotic cells (Fig. 7C and D, NC) in the *TaSBT1.7*-silenced plants was significantly smaller compared with that observed in BSMV::γ-treated leaves ($P < 0.05$). Importantly, the attenuated HR correlated with significantly increased hyphal lengths in the *TaSBT1*-silenced plants compared with control plants at 120 hpi ($P < 0.05$) (Fig. 7D). At 14 dpi, significant differences between *TaSBT1.7*-silenced plants and control plants in the *P. striiformis* f. sp. *tritici* biomass were also observed ($P < 0.05$) (Fig. 7E). Taken together, our observations indicate that the three *TaSBT1.7* homeologs serve an important function in HR activation and resistance against the biotrophic fungal pathogen *P. striiformis*.

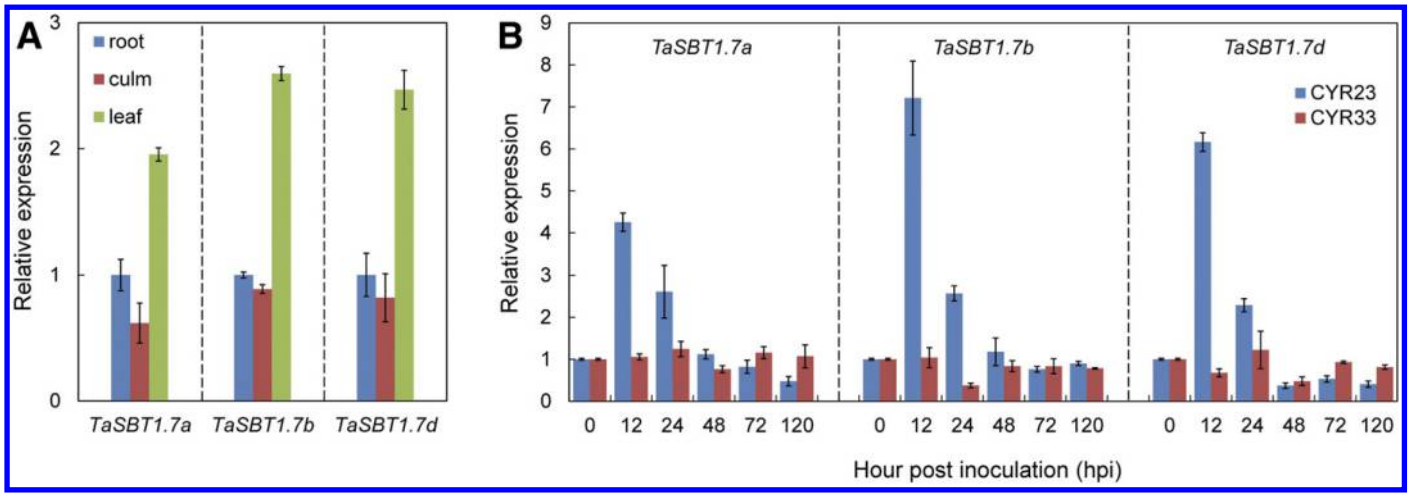

Fig. 4. Quantitative analyses of *SBT1.7* expressions in wheat. **A,** Expression of three *TaSBT1.7* homeologous in grain, root, culm, and leaf tissues of two-leaf-stage wheat plants. Expression levels were normalized to average activities (= 1) in roots. **B,** Expression of three *TaSBT1.7* homeologous upon inoculation of *Puccinia striiformis* f. sp. *tritici* with either avirulent strain CYR23 or virulent strain CYR33. Relative expression levels at the indicated time points were measured by quantitative reverse-transcription PCR. Data shown are the means ± standard deviation calculated from three independent biological replications.

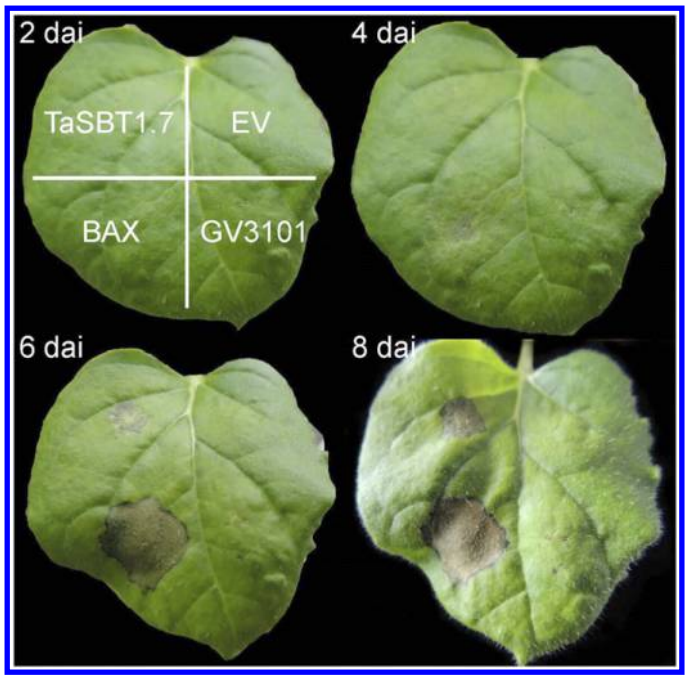

Fig. 5. Transient overexpression of *TaSBT1.7b* in *Nicotiana benthamiana* leaves. Leaves of *N. benthamiana* were infiltrated with agrobacterial cells (GV3101) transfected with the *pGR106* vector expressing *TaSBT1.7x* or *BAX* from the *35S* promoter, or the empty vector, or untransfected GV3101 cells. BAX is a death-promoting Bcl-2 family protein in animals that is capable of activating programmed cell death in many plants, including tobacco; dai = days after inoculation. Infiltrated leaves were photographed at the indicate time postinfiltration.

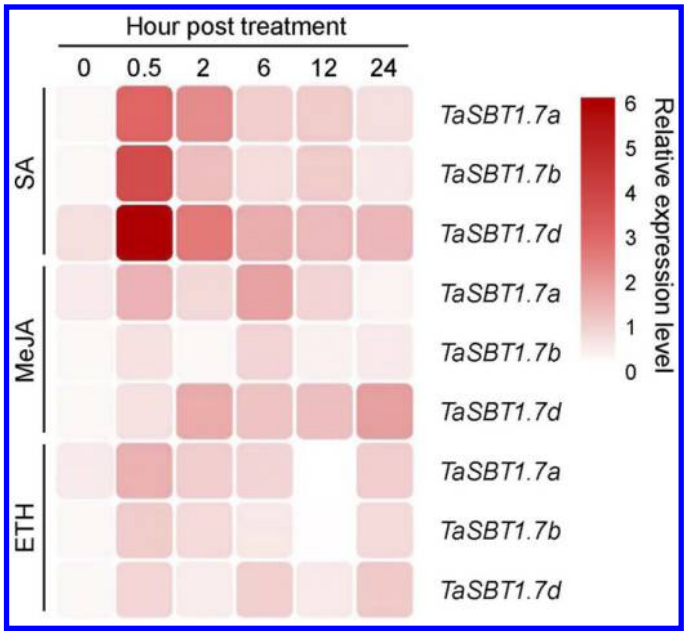

Fig. 6. Induction of *TaSBT1.7* by salicylic acid (SA) but not methyl jasmonic acid (MeJA) or ethylene (ETH). Two-leaf-stage wheat plants were sprayed with SA at 2 mmol/liter or MeJA at 100 µmol/liter, or treated with ETH at 100 µmol/liter (see Materials and Methods). Expression of the three *TaSBT1.7* homeologs were measured by quantitative reverse-transcription PCR at the indicated time points. Relative expression levels of *TaSBT1.7* homeologs were presented using the heatmap scale shown on the right. Experiments were repeated three times with similar results.

DISCUSSION

SBTs in the wheat genome. SBTs comprise a very diverse family of serine peptidases in many organisms, especially in plants (Figueiredo et al. 2018). To date, *SBT* gene families have been described in the genomes of *Arabidopsis* (*A. thaliana*) (Rautengarten et al. 2005), tomato (*Lycopersicon esculentum*) (Reichardt et al. 2018), rice (*Oryza sativa*) (Tripathi and Sowdhamini 2006), poplar (*Populus trichocarpa*) (Schaller et al. 2012), potato (*S. tuberosum*) (Norero et al. 2016), and grapevine (*Vitis vinifera*) (Figueiredo et al. 2016). The wheat genome contains 255 SBT-encoding genes, which constitutes the largest *SBT* gene family identified thus far in any given genome. This is not unexpected because the gigantic hexaploid wheat genome (15.4 to 15.8 Gb) contains the three subgenomes A, B, and D (The International Wheat Genome Sequencing Consortium et al. 2018), and there might have been more frequent local sequence duplication and diversification events during the evolution of the bread wheat genome (Shiu and Bleecker 2003). Notably, the TaSBT2 clade from the wheat genome contains 100 family members, suggesting that this clade has undergone remarkable gene amplification. The ratio of nonsynonymous (Ka) to synonymous (Ks) is a key indicator telling us the way the genes have evolved or been domesticated (Hurst 2002). The Ka/Ks value is much greater than 1 (the calculation result was 2.9575 using DnaSP software), showing strong evidence that positive selection has acted on the *TaSTB2* subfamily, which would further imply that these genes serve important and diverse physiological functions in wheat.

TaSBTs may be involved in defense regulation. Plant SBTs have been implicated in priming immune response against diverse pathogens. Such SBTs include tomato P69s (Tornero et al. 1996), oat Saspase-1 and Saspase-2 (Coffeen and Wolpert 2004), potato StSBTc-3 (Fernández et al. 2015), and *Arabidopsis* AtSBT3.3 (Ramírez et al. 2013). It was reported that tobacco NtPhytaspase may contribute to PCD associated with defense against tobacco mosaic virus and PCD caused by abiotic stresses (Chichkova et al. 2010, 2012). Similarly, StSBTc-3 was shown to have caspase-3-like activity that contributes to potato PCD associated with defense against *Phytophthora infestans* (Fernández et al. 2015). More convincing evidence for the involvement of am SBT in plant immunity was provided by Ramírez et al. (2013). They found that enhanced expression of AtSBT3.3 resulted in priming the SA-dependent defense response (Ramírez et al. 2013).

To identify TaSBTs that may serve a similar role in wheat immunity, we examined 67 candidate *TaSBT* genes whose expression

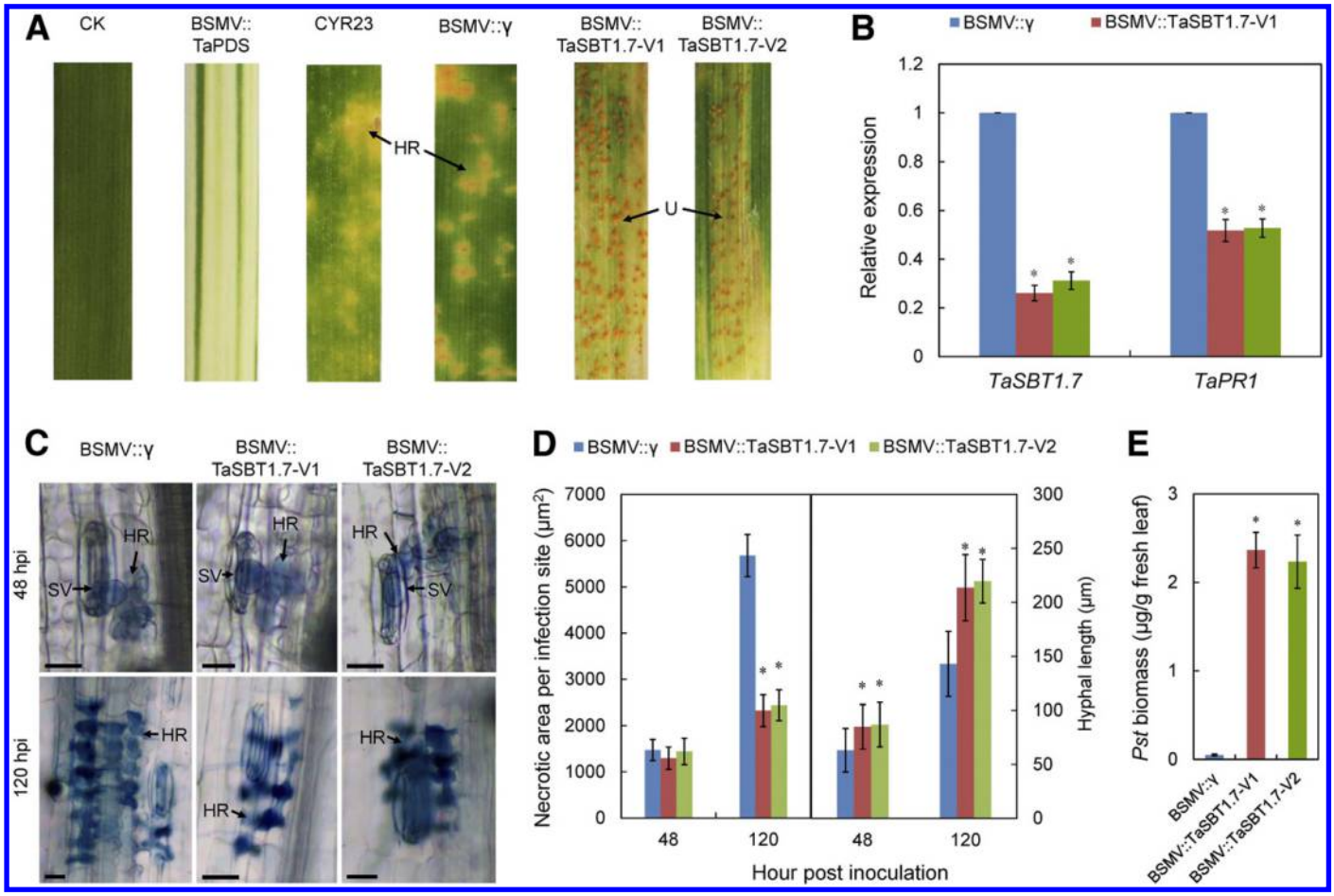

Fig. 7. Silencing *TaSBT1.7* by the barley stripe mosaic virus virus-induced gene silencing (*BSMV-VIGS*) system compromised resistance to an avirulent strain of stripe rust. **A,** Representative leaf segments of control plants (no treatment [CK], inoculated with avirulent strain CYR23, or infected with *BSMV::TaPDS*) and those infected with the *BSMV::*γ empty vector or *BSMV::TaSBT1.7-V1* or *BSMV::TaSBT1.7-V2* (see Materials and Methods for details) and inoculated with CYR23, an avirulent stain of *Puccinia striiformis* f. sp. *tritici*. Note: severe chlorosis was observed on the fourth leaves of the plants inoculated with *BSMV:TaPDS* at 12 days postinoculation (dpi) (which was the time for subsequent pathogen inoculation), indicating effective silencing of the target gene by this system. Disease symptoms of the fourth leaves of the plants were assessed and photographed at 14 dpi with CYR23. **B,** Relative transcript levels of *TaSBT1.7* and *TaPR1* in the fourth leaves of wheat plants infected with *BSMV* prior to inoculation with CYR23. **C,** Histological observation of host cell death in in the fourth leaves of *BSMV*-infected wheat plants at 48 and 120 h postinoculation (hpi) with CYR23. NC = necrotic cells stained by Trypan Blue and SV = substomatal vesicle. **D,** Areas of necrotic cell death (reflecting the degree of hypersensitive response) of in the fourth leaves of *BSMV*-infected wheat plants at 48 and 120 hpi with CYR23. At least 30 necrotic areas per samples were measured by the cellSens imaging software (Olympus). **E,** Biomass of *P. striiformis* f. sp. *tritici* measured at 14 dpi with CYR23. An asterisk (*) indicates significant difference ($P < 0.01$; Student's *t* test) compared with the empty vector control. Each experiment was repeated three times.

changed upon elicitor treatments or pathogen infection through mining of the public RNA-seq data. Among them, five *TaSBT* homeologous genes were induced by both PAMP elicitors and fungal pathogens (Fig. 3, stripes), suggesting that these genes may be involved in PAMP-triggered immunity or other defense mechanisms. Future genetic studies are required to clarify whether these *TaSBT* genes are, indeed, regulators of PCD and defense in wheat.

***TaSBT1.7* may play a role in defense signaling and HR.** Data from our previous and present studies suggest an important role for the *TaSBT1.7* homeologous genes (*TraesCS4A02G237500*, *TraesCS4B02G077600*, and *TraesCS4D02G076000*) in wheat defense against stripe rust caused by *Puccinia striiformis*. First, public RNA-seq data showed that all three *TaSBT1.7* homeologous genes were induced by PAMP elicitors or pathogens (Fig. 3; Supplementary Fig. S3), agreeing with our observations that these genes were upregulated in wheat during its incompatible interaction with *P. striiformis* (Fig. 4) (Yang et al. 2016). Second, transient overexpression of *TaSBT1.7* in *N. benthamiana* leaves resulted in necrotic cell death (Fig. 5). Currently, it is not known whether the cell death is due to activation of a relevant defense pathway in *N. benthamiana* or toxicity of *TaSBT1.7* to plant cells when it is above a certain threshold level. Finally, and more importantly, we found that silencing *TaSBT1.7* in wheat significantly compromised HR and resistance against *P. striiformis* (Fig. 6). It is interesting to note that, although no direct evidence has been reported for a role of the *Arabidopsis* homolog of *TaSBT1.7* in defense, AtSBT1.7 has been shown to inhibit the activity of PME by proteolysis (Ranocha et al. 2014; Rautengarten et al. 2008). Our findings also showed that higher PME activities in *TaSBT1.7* knock-down plants were detected compared with control plants (Supplementary Fig. S7), suggesting a possible role of *TaSBT1.7* in the modulation of PME activities in wheat. The plant cell wall is considered to be the "first obstacle" for pathogen invasion. As a main component of the plant primary cell wall, pectins or pectin-derived oligogalacturonides may play important roles in cell-wall-based immunity (Bacete et al. 2018). Indeed, loss of either *PMR5*, which encodes a pectin acetyltransferase (Chiniquy et al. 2019; Vogel et al. 2004), or *PMR6*, which encodes a pectin lyase, results in enhanced resistance to powdery mildew (Vogel et al. 2002). More recently, Liu et al. (2018) reported that ectopic expression of a pectin methylesterase inhibitor increased resistance in cotton to Verticillium wilt.

In summary, in this study, we conducted a detailed sequence analysis of all SBT-encoding genes from wheat, identified several candidate *TaSBTs* that may be involved in regulation of plant defense, and presented evidence for a positive role of *TaSBT1.7* in HR and resistance against the rust pathogen *P. striiformis*. Future research is required to identify the substrates of *TaSBT1.7* and understand how the induced expression of *TaSBT1.7* affects the defense signaling leading to HR and disease resistance.

LITERATURE CITED

Antão, C. M., and Malcata, F. X. 2005. Plant serine proteases: Biochemical, physiological and molecular features. Plant Physiol. Biochem. 43:637-650.

Arora, A., and Singh, V. 2004. Cysteine protease gene expression and proteolytic activity during floral development and senescence in ethylene-insensitive *Gladiolus grandiflora*. J. Plant Biochem. Biotechnol. 13: 123-126.

Bacete, L., Melida, H., Miedes, E., and Molina, A. 2018. Plant cell wall-mediated immunity: Cell wall changes trigger disease resistance responses. Plant J. 93:614-636.

Berger, D., and Altmann, T. 2000. A subtilisin-like serine protease involved in the regulation of stomatal density and distribution in *Arabidopsis thaliana*. Genes Dev. 14:1119-1131.

Borrill, P., Ramirez-Gonzalez, R., and Uauy, C. 2016. expVIP: A customizable RNA-seq data analysis and visualization platform. Plant Physiol. 170: 2172-2186.

Cai, Y.-m., and Gallois, P. 2015. Programmed cell death regulation by plant proteases with caspase-like activity. Pages 191-202 in: Plant Programmed Cell Death. A. Gunawardena and P. McCabe, eds. Springer, Cham, Switzerland.

Chen, C., Chen, H., Zhang, Y., Thomas, R. H., Frank, H. M., He, Y., and Xia, R. 2020. TBtools—An integrative toolkit developed for interactive analyses of big biological data. Mol. Plant 13:1194-1202.

Chichkova, N. V., Shaw, J., Galiullina, R. A., Drury, G. E., Tuzhikov, A. I., Kim, S. H., Kalkum, M., Hong, T. B., Gorshkova, E. N., and Torrance, L. 2010. Phytaspase, a relocalisable cell death promoting plant protease with caspase specificity. EMBO J. 29:1149-1161.

Chichkova, N. V., Tuzhikov, A. I., Taliansky, M., and Vartapetian, A. B. 2012. Plant phytaspases and animal caspases: Structurally unrelated death proteases with a common role and specificity. Physiol. Plant. 145:77-84.

Chiniquy, D., Underwood, W., Corwin, J., Ryan, A., Szemenyei, H., Lim, C. C., Stonebloom, S. H., Birdseye, D. S., Vogel, J., Kliebenstein, D., Scheller, H. V., and Somerville, S. 2019. PMR5, an acetylation protein at the intersection of pectin biosynthesis and defense against fungal pathogens. Plant J. 100:1022-1035.

Coffeen, W. C., and Wolpert, T. J. 2004. Purification and characterization of serine proteases that exhibit caspase-like activity and are associated with programmed cell death in *Avena sativa*. Plant Cell 16:857-873.

D'Erfurth, I., Le Signor, C., Aubert, G., Sanchez, M., Vernoud, V., Darchy, B., Lherminier, J., Bourion, V., Bouteiller, N., and Bendahmane, A. 2012. A role for an endosperm-localized subtilase in the control of seed size in legumes. New Phytol. 196:738-751.

Dodson, G., and Wlodawer, A. 1998. Catalytic triads and their relatives. Trends Biochem. Sci. 23:347-352.

Duan, X., Zhang, Z., Wang, J., and Zuo, K. 2016. Characterization of a novel cotton subtilase gene *GbSBT1* in response to extracellular stimulations and its role in *Verticillium resistance*. PLoS One 11:e0153988.

El-Gebali, S., Mistry, J., Bateman, A., Eddy, S. R., Luciani, A., Potter, S. C., Qureshi, M., Richardson, L. J., Salazar, G. A., and Smart, A. 2018. The Pfam protein families database in 2019. Nucleic Acids Res. 47: D427-D432.

Fan, T., Bykova, N. V., Rampitsch, C., and Xing, T. 2016. Identification and characterization of a serine protease from wheat leaves. Eur. J. Plant Pathol. 146:293-304.

Fernández, M. B., Daleo, G. R., and Guevara, M. G. 2012. DEVDase activity is induced in potato leaves during *Phytophthora infestans* infection. Plant Physiol. Biochem. 61:197-203.

Fernández, M. B., Daleo, G. R., and Guevara, M. G. 2015. Isolation and characterization of a *Solanum tuberosum* subtilisin-like protein with caspase-3 activity (StSBTc-3). Plant Physiol. Biochem. 86:137-146.

Figueiredo, A., Monteiro, F., and Sebastiana, M. 2014. Subtilisin-like proteases in plant-pathogen recognition and immune priming: A perspective. Front. Plant Sci. 5:739.

Figueiredo, J., Costa, G. J., Maia, M., Paulo, O. S., Malho, R., Silva, M. S., and Figueiredo, A. 2016. Revisiting *Vitis vinifera* subtilase gene family: A possible role in grapevine resistance against *Plasmopara viticola*. Front. Plant Sci. 7:1783.

Figueiredo, J., Sousa Silva, M., and Figueiredo, A. 2018. Subtilisin-like proteases in plant defence: The past, the present and beyond. Mol. Plant Pathol. 19:1017-1028.

Hein, I., Barciszewska-Pacak, M., Hrubikova, K., Williamson, S., Dinesen, M., Soenderby, I. E., Sundar, S., Jarmolowski, A., Shirasu, K., and Lacomme, C. 2005. Virus-induced gene silencing-based functional characterization of genes associated with powdery mildew resistance in barley. Plant Physiol. 138:2155-2164.

Hurst, L. D. 2002. The Ka/Ks ratio: Diagnosing the form of sequence evolution. Trends Genet. 18:486-487.

Jordá, L., Coego, A., Conejero, V., and Vera, P. 1999. A genomic cluster containing four differentially regulated subtilisin-like processing protease genes is in tomato plants. J. Biol. Chem. 274:2360-2365.

Jordá, L., and Vera, P. 2000. Local and systemic induction of two defense-related subtilisin-like protease promoters in transgenic Arabidopsis plants. Luciferin induction of PR gene expression. Plant Physiol. 124:1049-1058.

Liu, N. N., Sun, Y., Pei, Y. K., Zhang, X. Y., Wang, P., Li, X. C., Li, F. G., and Hou, Y. X. 2018. A pectin methylesterase inhibitor enhances resistance to *Verticillium Wilt*. Plant Physiol. 176:2202-2220.

Norero, N. S., Castellote, M. A., de la Canal, L., and Feingold, S. E. 2016. Genome-wide analyses of subtilisin-like serine proteases on *Solanum tuberosum*. Am. J. Potato Res. 93:485-496.

Othman, R., and Nuraziyan, A. 2010. Fruit-specific expression of papaya subtilase gene. J. Plant Physiol. 167:131-137.

Petty, I., French, R., Jones, R., and Jackson, A. 1990. Identification of barley stripe mosaic virus genes involved in viral RNA replication and systemic movement. EMBO J. 9:3453-3457.

Pfaffl, M. W. 2001. A new mathematical model for relative quantification in real-time RT-PCR. Nucleic Acids Res. 29:e45.

Ramírez, V., López, A., Mauch-Mani, B., Gil, M. J., and Vera, P. 2013. An extracellular subtilase switch for immune priming in Arabidopsis. PLoS Pathog 9:e1003445.

Ranocha, P., Francoz, E., Burlat, V., and Dunand, C. 2014. Expression of PRX36, PMEI6 and SBT1. 7 is controlled by complex transcription factor regulatory networks for proper seed coat mucilage extrusion. Plant Signal. Behav. 9:e977734.

Rautengarten, C., Steinhauser, D., Bussis, D., Stintzi, A., Schaller, A., Kopka, J., and Altmann, T. 2005. Inferring hypotheses on functional relationships of genes: Analysis of the *Arabidopsis thaliana* subtilase gene family. PLOS Comput. Biol. 1:e40.

Rautengarten, C., Usadel, B., Neumetzler, L., Hartmann, J., Büssis, D., and Altmann, T. 2008. A subtilisin-like serine protease essential for mucilage release from Arabidopsis seed coats. Plant J. 54:466-480.

Reichardt, S., Repper, D., Tuzhikov, A. I., Galiullina, R. A., Planas-Marques, M., Chichkova, N. V., Vartapetian, A. B., Stintzi, A., and Schaller, A. 2018. The tomato subtilase family includes several cell death-related proteinases with caspase specificity. Sci. Rep. 8:10531.

Roberts, I. N., Caputo, C., Kade, M., Criado, M. V., and Barneix, A. J. 2011. Subtilisin-like serine proteases involved in N remobilization during grain filling in wheat. Acta Physiol. Plant. 33:1997-2001.

Saez-Aguayo, S., Ralet, M. C., Berger, A., Botran, L., Ropartz, D., Marion-Poll, A., and North, H. M. 2013. PECTIN METHYLESTERASE INHIBITOR6 promotes Arabidopsis mucilage release by limiting methylesterification of homogalacturonan in seed coat epidermal cells. Plant Cell 25:308-323.

Schaller, A., Stintzi, A., and Graff, L. 2012. Subtilases—Versatile tools for protein turnover, plant development, and interactions with the environment. Physiol. Plant. 145:52-66.

Schaller, A., Stintzi, A., Rivas, S., Serrano, I., Chichkova, N. V., Vartapetian, A. B., Martínez, D., Guiamét, J. J., Sueldo, D. J., and Van Der Hoorn, R. A. 2018. From structure to function—A family portrait of plant subtilases. New Phytol. 218:901-915.

Shiu, S.-H., and Bleecker, A. B. 2003. Expansion of the receptor-like kinase/Pelle gene family and receptor-like proteins in Arabidopsis. Plant Physiol. 132:530-543.

Tanaka, H., Onouchi, H., Kondo, M., Hara-Nishimura, I., Nishimura, M., Machida, C., and Machida, Y. 2001. A subtilisin-like serine protease is required for epidermal surface formation in Arabidopsis embryos and juvenile plants. Development 128:4681-4689.

Taylor, A., and Qiu, Y.-L. 2017. Evolutionary history of subtilases in land plants and their involvement in symbiotic interactions. Mol. Plant-Microbe Interact. 30:489-501.

The International Wheat Genome Sequencing Consortium. 2014. A chromosome-based draft sequence of the hexaploid bread wheat (*Triticum aestivum*) genome. Science 345:1251788.

The International Wheat Genome Sequencing Consortium. 2018. Shifting the limits in wheat research and breeding using a fully annotated reference genome. Science 361:eaar7191.

Tornero, P., Conejero, V., and Vera, P. 1996. Primary structure and expression of a pathogen-induced protease (PR-P69) in tomato plants: Similarity of functional domains to subtilisin-like endoproteases. Proc. Natl. Acad. Sci. U.S.A. 93:6332-6337.

Tornero, P., Conejero, V., and Vera, P. 1997. Identification of a new pathogen-induced member of the subtilisin-like processing protease family from plants. J. Biol. Chem. 272:14412-14419.

Tripathi, L. P., and Sowdhamini, R. 2006. Cross genome comparisons of serine proteases in Arabidopsis and rice. BMC Genomics 7:200.

van der Hoorn, R. A. L. 2008. Plant proteases: From phenotypes to molecular mechanisms. Annu. Rev. Plant Biol. 59:191-223.

Vogel, J. P., Raab, T. K., Schiff, C., and Somerville, S. C. 2002. PMR6, a pectate lyase-like gene required for powdery mildew susceptibility in Arabidopsis. Plant Cell 14:2095-2106.

Vogel, J. P., Raab, T. K., Somerville, C. R., and Somerville, S. C. 2004. Mutations in PMR5 result in powdery mildew resistance and altered cell wall composition. Plant J. 40:968-978.

Wang, B., Sun, Y. F., Song, N., Zhao, M. X., Liu, R., Feng, H., Wang, X. J., and Kang, Z. S. 2017. *Puccinia striiformis* f. sp. *tritici* microRNA-like RNA 1 (Pst-milR1), an important pathogenicity factor of *Pst*, impairs wheat resistance to *Pst* by suppressing the wheat pathogenesis-related 2 gene. New Phytol. 215:338-350.

Wulff, B. B., and Dhugga, K. S. 2018. Wheat—The cereal abandoned by GM. Science 361:451-452.

Xu, Y., Wang, S., Li, L., Sahu, S. K., Petersen, M., Liu, X., Melkonian, M., Zhang, G., and Liu, H. 2019. Molecular evidence for origin, diversification and ancient gene duplication of plant subtilases (SBTs). Sci. Rep. 9:12485.

Yang, Y., Yu, Y., Bi, C., and Kang, Z. 2016. Quantitative proteomics reveals the defense response of wheat against *Puccinia striiformis* f. sp. *tritici*. Sci. Rep. 6:34261.

Yang, Y., Zhao, J., Liu, P., Xing, H., Li, C., Wei, G., and Kang, Z. 2013. Glycerol-3-phosphate metabolism in wheat contributes to systemic acquired resistance against *Puccinia striiformis* f. sp. *tritici*. PLoS One 8: e81756.

Yu, Y., Xiao, J. F., Zhu, W. J., Yang, Y. H., Mei, J. Q., Bi, C. W., Qian, W., Qing, L., and Tan, W. Z. 2017. Ss-Rhs1, a secretory Rhs repeat-containing protein, is required for the virulence of *Sclerotinia sclerotiorum*. Mol. Plant Pathol. 18:1052-1061.

Zhao, C., Johnson, B. J., Kositsup, B., and Beers, E. P. 2000. Exploiting secondary growth in Arabidopsis. Construction of xylem and bark cDNA libraries and cloning of three xylem endopeptidases. Plant Physiol. 123: 1185-1196.

Zhou, T., Li, J., Yang, L., Ruan, R., Yang, Y., and Li, Z. 2020. The Resistance Prediction of Wheat Hybrids Based on the Sensibility of Their Parents to Stripe Rust. Sci. Agric. Sin. 53:1806-1819.